ROTATIONAL SPECTRUM AND HYPERFINE STRUCTURE OF THE $^2\Sigma$ RADICALS BaF AND BaCl

Ch. RYZLEWICZ, H.-U. SCHÜTZE-PAHLMANN, J. HOEFT and T. TÖRRING

Institut für Molekülphysik, Freie Universität Berlin, D-1000 Berlin 33, West Germany

Microwave rotational spectra have been measured for BaF and BaCl. Precise Dunham coefficients Y_{ik} and spin–rotation parameters γ_{ik} are derived from this first rotational analysis for the BaCl molecule. Hyperfine structure has been measured for the isotopes $^{137}\text{Ba}^{19}\text{F}$ and $^{137}\text{Ba}^{35}\text{Cl}$ in which coupling of two nuclei has to be considered. Matrix elements for calculation of energy levels and relative intensities are given in the text. The measured hfs coupling constants are: $b(^{137}\text{Ba}) = 2301(9)$ MHz, $c(^{137}\text{Ba}) = 75(6)$ MHz, $eqQ(^{137}\text{Ba}) = -117(12)$ MHz, and $b(^{19}\text{F}) = 60(6)$ MHz. A comparison between these first gas phase measurements of metal hfs coupling constants in group II monohalides with previous matrix ESR data and hfs splitting factors A and B in the free Ba^+ ion yields information about polarization of closed Ba shells and 6s-6p-5d hybridization of the unpaired electron due to the field of the F^- ion.

1. Introduction

Spectra of earth alkaline monohalides have been investigated by various spectroscopic techniques during the recent years. These investigations have provided for the first time detailed and precise information on $^2\Sigma$ radicals in many rotational and vibrational states. Complementary information is obtained by the different experimental techniques. Vibrational and rotational constants have been measured by laser-induced fluorescence and excitation spectra [1–5]. Even spin-doubling, formerly referred to as ρ-doubling, and hyperfine splittings have been resolved in the optical region by Doppler-free methods like intermodulated fluorescence [6,7], saturation spectroscopy [8] and optical polarization spectroscopy [9] in some cases. The accuracy of molecular parameters determined from optical spectra usually suffers from correlations between upper state–lower state constants [10]. These correlations can be broken nearly completely if rotational spectra in the electronic ground state have been measured independently [10,11]. Such measurements have been made by microwave–optical double resonance (MODR) [12–14] and microwave absorption spectroscopy [15–17]. Even finer details like vibrational and rotational dependence of spin-doubling and

hyperfine constants have been studied by molecular beam radio frequency–optical double resonance (MBDR) [18–21].

Hyperfine structure from the halogen atom is present in all molecules of this group and has been measured for the Ca-halides and for SrF by optical and MBDR techniques [7,18–21]. Like previous matrix ESR experiments [22], these results confirm that the chemical bond in the earth alkaline monohalides is highly ionic. From this reason the hfs splitting in the pure rotational spectrum is very small and has not been resolved yet by MODR or microwave spectroscopy. However, it has been demonstrated that effects of unresolved hyperfine structure have to be considered in the interpretation of microwave spectra even if no inhomogeneous line broadening is observed, since systematic line shifts may occur [16]. Very recently it has become possible to observe rotational transitions $N = 1 \leftarrow 0$ and $N = 2 \leftarrow 1$ with well-resolved hyperfine structure for CaCl with the new technique of microwave–optical polarization spectroscopy (MOPS) [9,23].

The direct investigation of charge and spin density distribution in the metal atom of these molecules by measuring the metal hyperfine structure is largely impeded by the fact that only a few isotopes with relatively small natural abundance have a non-zero spin

and that the spin quantum number in most of these cases is rather high. So only ESR matrix spectra have been reported for ^{87}SrF and ^{137}BaF in which isotopically enriched samples have been used [22]. These measurements resulted in the expected large Fermi contact interaction for the unpaired electron but also showed a relatively high anisotropy in the magnetic interaction indicating that the unpaired outer orbital electron is highly hybridized due to the field of the near by F$^-$ ion. The experiments described here for the isotopic species ^{137}Ba^{19}F and ^{137}Ba^{35}Cl provide the first gas-phase measurements of these magnetic coupling constants. In addition they give the quadrupole coupling constant of ^{137}Ba in these molecules. Because of the highly ionic bond the electric field gradient at the ^{137}Ba nucleus is due to a single unpaired valence shell electron and polarization of the closed electronic shells. These two effects can be clearly separated since the contribution of the unpaired electron to the eqQ value can be calculated from the measured c value when the nuclear magnetic moment and the electric quadrupole moment are known. The amount of 6p and 5d hybridization of the unpaired 6s valence electron can then be calculated by a comparison with experimentally determined hyperfine coupling constants in the ^{2}S, ^{2}P, and ^{2}D states of the ^{137}Ba$^+$ ion [24].

Hyperfine structure for the halogen nucleus was partly resolved in the ^{137}BaF spectrum and had to be considered also in the interpretation of the ^{137}BaCl spectrum. It was therefore necessary to include magnetic and electric coupling of both nuclei in the hamiltonian. Since to our best knowledge no matrix elements for this case have been published yet these have been calculated and are given in section 3.

2. Experimental

In view of the relatively large amount of substance needed for microwave spectroscopy of high-temperature species all experiments had to be done with samples of natural isotopic abundance. Although ^{137}Ba with spin $I = 3/2$ and a natural abundance of 11.3% is a favourable case for hyperfine structure measurements among group IIa halides, sensitivity is the most crucial point in these experiments. This is true because the concentration which can be obtained in the absorption cell for these chemically unstable species is about a fac-

tor of 100 less than for chemically stable molecules, e.g. BaO [15]. Measurements are thus restricted to the mm range where absorption coefficients are large. Measurements have been carried out in the region around 100 GHz and 280 GHz where some Varian klystrons and a Thomson CSF backward wave oscillator were available. A simplified block diagram of the spectrometer is shown in fig. 1. Stable phase locking of the 300 GHz BWO to the 1 GHz output of the frequency standard requires two phase lock loops with a second BWO locked at an intermediate frequency of ≈30 GHz. For the measurement of single lines the 300 GHz BWO can be swept electronically over a range of a few MHz by sweeping the reference frequency of the synchronizer. Large frequency intervals can be scanned by tuning the frequency standard. In both cases frequency markers can be displayed along with the measured spectrum which is not shown in fig. 1.

Molecules are produced in a free space absorption cell in a low-pressure flame [15]. Ba metal evaporated from a small crucible and entrained in a stream of argon buffer gas is mixed at room temperature with IF$_5$ or Cl$_2$ to produce BaF or BaCl, respectively, in an exothermic reaction. The total cell pressure is ≈0.05 Torr. Although the pressure of the oxidizing gas is rather critical this production scheme has proved to be very convenient for these molecules and stable conditions can be maintained for hours.

The free space absorption cell consists of commercially available glass pipes of 15 cm diameter. The total length of the cell is 100 cm. Production of the molecules can be monitored by looking at the chemiluminescence with a small monochromator. Microwave radiation is fed through the cell by horns and lenses. The detector is a helium-cooled commercial IR detector
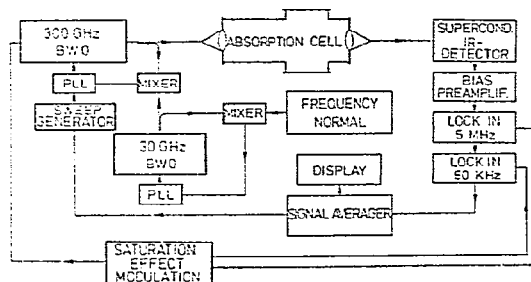

Fig. 1. Block diagram of the 300 GHz spectrometer.

(Advanced Kinetics, Inc.). The In–Sb photoconductive crystal has a fast response time which is essential for the application of saturation effect modulation [25]. Using this technique for separation of the signal from the mw background, signal output of the detector is at 5.05 MHz and 4.95 MHz with fixed phase relations between these two frequencies. In a first lock-in with a reference frequency of 5 MHz this signal is converted to 50 kHz which is further amplified in a second lock-in. Signal averaging can be used for the detection of weak lines. However, useful integration times are limited to only a few minutes since suppression of baseline fluctuations by saturation modulation is not complete.

The same spectrometer has been used for the 100 GHz measurements. The 300 GHz BWO was then replaced by a klystron.

3. Theory

The earth alkaline halides in their $^2\Sigma$ ground state are good examples of Hund's case b radicals. The effective hamiltonian for the analysis of the rotational spectrum may be written as

$$\hat{H} = B\hat{N}^2 + \gamma\hat{N}\cdot\hat{S} + \hat{H}_{hfs}, \tag{1}$$

where the first and second term describe the rotational energy and the effective electron-spin rotation interaction, respectively, and the third term summarizes all effects in which nuclear spins are involved. Matrix elements are calculated in the representation $|(NS)JI_1F_1I_2FM_F\rangle$. In this coupling, which corresponds to Hund's case $b_{\beta J}$ [26] matrix elements of the two first terms in (1) are diagonal in all quantum numbers (summarized by x)

$$\langle x|B\hat{N}^2|x\rangle = BN(N+1),$$

$$\langle x|\gamma\hat{N}\cdot\hat{S}|x\rangle = \tfrac{1}{2}\gamma N, \qquad \text{for } J = N + \tfrac{1}{2};$$

$$= -\tfrac{1}{2}\gamma(N+1), \qquad \text{for } J = N - \tfrac{1}{2}. \tag{2}$$

$\hat{H}_{hfs}$ is given by the magnetic hyperfine structure hamiltonian of Frosch and Foley [27] supplemented by terms to include nuclear spin–rotation and electric quadrupole interaction. For one coupling nucleus we have

$$\hat{H}_{hfs} = b\hat{I}\cdot\hat{S} + c\hat{I}_z\,\hat{S}_z + C_I\hat{I}\cdot\hat{N}$$

$$+ eqQ\,[3\hat{I}_z^2 - I(I+1)]/4I(2I-1). \tag{3}$$

Corresponding terms have to be added for the second nucleus. For the evaluation of matrix elements it is convenient to rewrite $\hat{H}_{hfs}$ in terms of spherical tensor operators so that standard operator techniques [28] can be used in the calculations. Doing this we get the matrix elements listed in table 1. For the analysis of the complex spectra it is often useful or even neccessary to known accurate relative intensities of all components of the $N + 1 \leftarrow N$ transition. Matrix elements of relative transition moments are therefore included in table 1. The total transition strength of $N + 1 \leftarrow N$ transition has been normalized to 1 in these expressions. For low-N transitions the first-order intensities given directly by the square of these matrix elements are often not adequate. This is true since hyperfine splitting can be of the same order of magnitude as the γ splittings. Then the transition matrix must be transformed by means of a similarity transformation to the basis which diagonalizes the hamiltonian. The correct relative intensities are given by the squares of the elements of the transformed matrix.

The matrix elements in table 1 are written in terms of (3j)-, (6j)-, and (9j)-symbols. For one coupling nucleus, elements in explicit form have been calculated by Radford [29]. In this case the energy matrix can be factorized into a set of 2 × 2 matrices if elements non-diagonal in N can be neglected, and relatively simple explicit expressions for the energy levels can be obtained. Using algebraic tables for the (nj)-symbols [30] it can easily be shown that the matrix elements given here are in agreement with Radford's results, except an obvious misprint in Radford's paper, which has already been pointed out by Bernath [7]. For two coupling nuclei the energy submatrices become larger and numerical matrix diagonalization has to be employed. It then seems more convenient to use matrix elements in the compact form provided by the (nj)-symbols and to evaluate the numerical values of these symbols by computer subroutines.

The molecular parameters in the effective hamiltonian (1) are functions of the internuclear distance and therefore depend on the vibrational and rotational state. We adopt here the notation of Childs et al. [18] who write the dependence for an arbitrary molecular pa-

Table 1

Matrix elements of $\hat{H}_{hfs}$ and of relative transition moments in the basis $|(NS)JI_1F_1I_2FM_F\rangle$. The abbreviations $\langle\|Q\|\rangle = \langle Q\|Q\|Q\rangle$ $= [Q(Q+1)(2Q+1)]^{1/2}$ and $[P,Q,...,T] = (2P+1)(2Q+1)...(2T+1)$ have been used throughout

Interaction	Matrix element
Fermi contact	$(b_1+\tfrac{1}{3}c_1)(-1)^t[J,J']^{1/2}\langle\|S\|\rangle\langle\|I_2\|\rangle \begin{Bmatrix} J' & S & N \\ S & J & 1 \end{Bmatrix} \begin{Bmatrix} F_1 & J' & I_1 \\ 1 & I_1 & J \end{Bmatrix} \delta_{NN'}\delta_{F_1F_1'}$
	with $t=N+S+J+J'+I_1+F_1+1$
	$(b_2+\tfrac{1}{3}c_2)(-1)^t[F_1,F_1',J,J']^{1/2}\langle\|S\|\rangle\langle\|I_2\|\rangle \begin{Bmatrix} J' & S & N \\ S & J & 1 \end{Bmatrix} \begin{Bmatrix} F_1' & J' & I_1 \\ J & F_1 & 1 \end{Bmatrix} \begin{Bmatrix} F & F_1' & I_2 \\ 1 & I_2 & F_1 \end{Bmatrix} \delta_{NN'}$
	with $t=N+S+2J+I_1+I_2+2F_1'+F$
dipolar spin–spin	$(10/3)^{1/2}c_1(-1)^t[N,N',J,J']^{1/2}\langle\|S\|\rangle\langle\|I_1\|\rangle \begin{pmatrix} N' & 2 & N \\ 0 & 0 & 0 \end{pmatrix} \begin{Bmatrix} F_1 & J' & I_1 \\ 1 & I_1 & J \end{Bmatrix} \begin{Bmatrix} N & N' & 2 \\ S & S & 1 \\ J & J' & 1 \end{Bmatrix} \delta_{F_1F_1'}$
	with $t=N+J'+I_1+F_1+1$
	$(10/3)^{1/2}c_2(-1)^t[N,N',J,J',F_1F_1']^{1/2}\langle\|S\|\rangle\langle\|I_2\|\rangle \begin{pmatrix} N' & 2 & N \\ 0 & 0 & 0 \end{pmatrix} \begin{Bmatrix} F_1' & J' & I_1 \\ J & F_1 & 1 \end{Bmatrix} \begin{Bmatrix} F & F_1' & I_2 \\ 1 & I_2 & F_1 \end{Bmatrix} \begin{Bmatrix} N & N' & 2 \\ S & S & 1 \\ J & J' & 1 \end{Bmatrix}$
	with $t=N+J+2F_1'+I_1+I_2+F$
Nuclear spin–rotation	$(c_I)_1(-1)^t[J,J']^{1/2}\langle\|N\|\rangle\langle\|I_1\|\rangle \begin{Bmatrix} J' & N & S \\ N & J & 1 \end{Bmatrix} \begin{Bmatrix} F_1 & J' & I_1 \\ 1 & I_1 & J \end{Bmatrix} \delta_{NN'}\delta_{F_1F_1'}$
	with $t=N+S+2J'+I_1+F_1+1$
	$(c_I)_2(-1)^t[F_1,F_1',J,J']^{1/2}\langle\|N\|\rangle\langle\|I_2\|\rangle \begin{Bmatrix} J' & N & S \\ N & J & 1 \end{Bmatrix} \begin{Bmatrix} F_1' & J' & I_1 \\ J & F_1 & 1 \end{Bmatrix} \begin{Bmatrix} F & F_1' & I_2 \\ 1 & I_2 & F_1 \end{Bmatrix} \delta_{NN'}$
	with $t=N+S+J+J'+I_1+I_2+2F_1'+F$
electric quadrupole	$\tfrac{1}{4}(eqQ)_1(-1)^t[N,N',J,J']^{1/2}\begin{pmatrix} N' & 2 & N \\ 0 & 0 & 0 \end{pmatrix} \begin{pmatrix} I_1 & 2 & I_1 \\ -I_1 & 0 & I_1 \end{pmatrix}^{-1} \begin{Bmatrix} J' & N' & S \\ N & J & 2 \end{Bmatrix} \begin{Bmatrix} F_1 & J' & I_1 \\ 2 & I_1 & J \end{Bmatrix} \delta_{F_1F_1'}$
	with $t=S+2J'+I_1+F_1$
	$\tfrac{1}{4}(eqQ)_2(-1)^t[N,N',J,J',F_1,F_1']^{1/2}\begin{pmatrix} N' & 2 & N \\ 0 & 0 & 0 \end{pmatrix} \begin{pmatrix} I_2 & 2 & I_2 \\ -I_2 & 0 & I_2 \end{pmatrix}^{-1} \begin{Bmatrix} J' & N' & S \\ N & J & 2 \end{Bmatrix} \begin{Bmatrix} F_1' & J' & I_1 \\ J & F_1 & 2 \end{Bmatrix} \begin{Bmatrix} F & F_1' & I_2 \\ 2 & I_2 & F_1 \end{Bmatrix}$
	with $t=S+J+J'+I_1+I_2+2F_1'+F$
relative transition moments	$(-1)^t[S_1,I_1,I_2]^{-1/2}[J,J',F_1F_1',F,F']^{1/2} \begin{Bmatrix} J' & N'S \\ N & J & 1 \end{Bmatrix} \begin{Bmatrix} F_1' & J' & I_1 \\ J & F_1 & 1 \end{Bmatrix} \begin{Bmatrix} F' & F_1' & I_2 \\ F_1 & F & 1 \end{Bmatrix}$
	with $t=N+S+J+J'+I_1+F_1+F_1'+I_2+F'+1$

rameter X_{vN} as a Dunham-type [31,32] double series in powers of $v+\tfrac{1}{2}$ and $N(N+1)$:

$$X_{vN} = \sum_{i,k} X_{ik}(v+\tfrac{1}{2})^i N^k (N+1)^k. \qquad (4)$$

When this expression is applied to the rotational constant B_{vN} the resulting B_{ik} are related to the usual

Dunham coefficients of the rotation–vibration energy by

$$B_{ik} = Y_{i(k+1)}. \qquad (5)$$

The X_{ik} of different isotopic species differ because of the different reduced masses and — for some of the constants — because of different nuclear moments. The ratio of the constants for two isotopes labeled by

the superscripts 1 and 2 can be written as

$$X_{ik}^1/X_{ik}^2 = \theta\,(\mu^1/\mu^2)^{-(1+2m+\lambda)/2}, \qquad (6)$$

where μ^1 and μ^2 stand for the reduced masses of the two isotopes. The quantity λ is 2 if X_{vN} refers to B, γ, or c_I, and 0 if X_{vN} refers to the hyperfine parameters b, c, or eqQ. The factor θ is unity for B and γ, but equals the ratio of the nuclear dipole moments for b, c, or c_I, and of the quadrupole moments if X_{vN} refers to the quadrupole parameter eqQ.

In previous papers [15,16] we have described the spin–rotation parameter γ by γ_e, α_γ and δ_γ. These are related to the γ_{ik} defined by (4) as: $\gamma_e \equiv \gamma_{00}$; $\alpha_\gamma \equiv \gamma_{10}$; $\delta_\gamma \equiv \gamma_{01}$.

4. Results

4.1. Hyperfine structure in $^{137}Ba^{19}F$

The microwave rotational spectrum of the most abundant isotope $^{138}Ba^{19}F$ and a few transitions of $^{136}Ba^{19}F$ have been reported in a previous paper [15]. From these data the Dunham coefficients Y_{ik} and the γ constant of $^{137}Ba^{19}F$ can be calculated using relations (4)–(6). Taking these constants and the hyperfine structure parameters from the matrix ESR measurements of Knight et al. [22] preliminary calculations of the spectrum can be made. Because of the strong Fermi contact interaction between S and I_{Ba} angular momentum coupling in the molecule is near to Hund's case b_{β_s} for low rotational states and approaches case b_{β_J} for high N values. For the transitions considered here we have intermediate coupling and J is not a good quantum number. Coupling of the fluorine nucleus is weak so that F_1 remains rather well defined and energy levels may be labeled by F, F_1 and N. By far the strongest transitions and the only ones which can be observed in the present experiment have selection rules $\Delta F = \Delta F_1 = \Delta N = +1$. The calculations show that all hyperfine components will be located within a frequency range of $\pm\,\gamma/2$ around the position of the hypothetical unsplit transition frequency $N+1 \leftarrow N$, so only this relatively small frequency range has to be scanned with high sensitivity in searching for lines. The transition is expected to consist of $(2S+1)(2I_{Ba}+1) = 8$ lines which are further split into doublets by the interaction with the fluorine nucleus with $I_F = 1/2$. It

can be seen from table 2 that not all these lines have been measured. For example, in the transition $N = 22 \leftarrow 21$ the second doublet with $F_1 = 21 \leftarrow 20$ near 284874.6 MHz is missed. This is due to an accidental overlap of signals produced by the saturation modulation technique. Using this technique each absorption line will appear twice in the spectrum [25] with a frequency difference which is 10 MHz in our apparatus. Thus the missed line will show overlap with the doublets around 284884.4 and 284864.6 MHz. Accidental overlap is even worse for the $N = 8 \leftarrow 7$ transition. In principle this can be avoided by using other modulation frequencies in the saturation effect modulation scheme. However, in our apparatus the frequency distance for the appearance of the two signals from one transition can be reduced only to 9 MHz. This turned out to be not sufficient for a clear separation of all lines.

The measured transition frequencies have been fitted to the hamiltonian for two coupling nuclei in a non-lin-

Table 2
Transition frequencies $N+1 \leftarrow N$, $F_1+1 \leftarrow F_1$, $F+1 \leftarrow F$ of $^{137}Ba^{19}F$ in the ground vibrational state $v = 0$

N	F	F_1	Obs. (MHz)	Calc. (MHz)	Obs. −calc. (kHz)
7	5.5	5 }	103 622.922	{ 103 622.985 103 623.051	−96
7	4.5	5			
7	8.5	8	103 639.592	103 639.542	50
7	7.5	8	103 639.892	103 639.866	26
7	5.5	6	103 648.221	103 648.186	35
7	6.5	6	103 648.521	103 648.512	9
7	7.5	8 }	103 687.323	{ 103 687.242 103 687.467	−32
7	8.5	8			
7	9.5	9 }	103 703.963	{ 103 703.950 103 703.983	−4
7	8.5	9			
21	19.5	19 }	284 829.132	{ 284 829.079 284 829.086	50
21	18.5	19			
21	22.5	22 }	284 840.730	{ 284 840.623 284 840.831	3
21	21.5	22			
21	21.5	21	284 854.732	284 854.775	−43
21	20.5	21	284 855.132	284 855.196	−64
21	19.5	20	284 864.420	284 864.461	−41
21	20.5	20	284 864.920	284 865.040	−120
21	20.5	21	284 884.170	284 884.151	19
21	21.5	21	284 884.620	284 884.559	61
21	21.5	22	284 898.434	284 898.527	−93
21	22.5	22	284 898.814	284 898.723	91
21	23.5	23 }	284 910.218	{ 284 910.256 284 910.261	−41
21	22.5	23			

ear least-squares fit. Lines from unresolved doublets
have been fitted to the theoretical doublet center. In
view of the large numbers of parameters which have
small and competing influence on transition frequen-
cies great care must be taken and none of the param-
eters should be neglected in the fit without studying
possible effects on the other constants. This is especial-
ly true since only two rotational transitions have been
measured. The rotational constant and the spin—rota-
tion constant γ have been included in the fit. The con-
sistency of these fitted values with those obtained via
mass relations from the ^{138}BaF data may serve as an
additional test for the reliability of the fit. Results are
listed in table 3. The parameters are effective param-
eters for the ground vibrational state for which the fol-
lowing abbreviations have been used:

$$B_0 = Y_{01} + \tfrac{1}{2} Y_{11} + \tfrac{1}{4} Y_{21},$$

$$D_0 = -(Y_{02} + \tfrac{1}{2} Y_{12}),$$

$$\gamma_0 = \gamma_{00} + \tfrac{1}{2} \gamma_{10} = \gamma_e + \tfrac{1}{2} \alpha_\gamma,$$

$$\delta_\gamma = \gamma_{01}. \qquad (7)$$

The agreement between fitted values and those derived
from mass relations is surprisingly good. Inclusion of
c_2 and of the nuclear spin—rotation constant c_I for the
Ba nucleus in the fit gave these constants with a more
than 100% error without any significant influence on
the other constants. Agreement between observed and
calculated frequencies in table 2 is also very good in
view of the very poor signal-to-noise ratio of all lines.
The hyperfine structure parameters given in table 3 may
therefore be considered as well determined.

Table 3
Molecular parameters for ^{137}Ba^{19}F

	Fitted parameters (MHz)	From ^{138}BaF [15] and mass relations[a] (MHz)
B_0	6479.6773(32)	6479.6734(17)
D_0	0.005544(3)	0.005540(1)
γ_0	81.025(220)	81.026(20)
δ_γ	0.000113(147)	0.000112(17)
b_1	2301(9)	
c_1	75(6)	
$(eqQ)_1$	−117(12)	
b_2	60(6)	

[a] Atomic masses from ref. [34].

4.2. Rotational spectrum and hyperfine structure of BaCl

No rotational analysis has been published for the
BaCl molecule yet. Extrapolations of rotational con-
stants from bond length in other molecules will usually
have an error of $\approx 1\%$. This means that essentially no
useful prediction of the spectrum can be made in the
300 GHz range and large spectral ranges have to be
searched. Results for the isotopic species ^{138}Ba^{35}Cl,
^{138}Ba^{37}Cl, and ^{136}Ba^{35}Cl are listed in table 4. All hy-
perfine structure effects may be neglected in fitting
these lines. Magnetic nuclear moments of both chlorine
isotopes are more than a factor of 3 smaller than in
fluorine and electric quadrupole moments are also very
small [33]. Since chemical bonding in BaF and BaCl is
very much the same the magnetic coupling constants
can be estimated as $b_{Cl} < 20$ MHz, $c_{Cl} < 5$ MHz. Pre-
liminary calculations showed that no measurable line
shifts are to be expected from coupling constants of
this order of magnitude for the measured lines. The
measured transition frequencies for ^{138}Ba^{35}Cl have
thus been fitted with a linear least-squares fit program
to the Dunham parameters and the spin—rotation inter-
action constants. Since rather high N quantum numbers
are involved, the Dunham parameter Y_{03} was included
but with its value kept fixed to the other constants ac-
cording to [33]:

$$Y_{03} = 2 Y_{02}^2/Y_{01} + \tfrac{1}{3} Y_{11}(-Y_{02}/Y_{01})^{3/2}. \qquad (8)$$

The results of this fit are given in table 5. Using these
constants and mass relations the transition frequencies
of the ^{136}Ba^{35}Cl lines have been calculated. As can be
seen from table 4 the agreement is excellent. All devia-
tions between observed and calculated frequencies are
well within the estimated experimental uncertainties
of ≈ 30 kHz.

The situation is different for ^{138}Ba^{37}Cl. Here the
agreement was poor and $Y_{01} = 2408.78762(21)$ MHz
from mass relations had to be changed to Y_{01}
$= 2408.79172(43)$ MHz in order to obtain a good fit.
Similar deviations from mass relations have been report-
ed for SrCl [17] and CaCl [16] while no such effects
have been observed for bromine isotopic substitution
in CaBr [16] and for barium substitution in BaF [15]
and in the BaCl measurements reported in this work.
As can be seen from table 6 half of the effect can be
explained by considering the highly ionic bond charac-

Table 4

Transition frequencies $N+1 \leftarrow N, J+1 \leftarrow J$ for the isotopic species $^{138}Ba^{35}Cl$, $^{138}Ba^{37}Cl$, and $^{136}Ba^{35}Cl$

Isotope	N	J	v	Obs. (MHz)	Obs. −calc. (kHz)
$^{138}Ba^{35}Cl$	20	19.5	0	105 456.630	−12
	20	20.5	0	105 506.283	6
	20	20.5	1	105 085.705	−7
	20	19.5	2	104 616.590	9
	20	20.5	2	104 665.685	−1
	53	52.5	0	270 728.238	11
	53	53.5	0	270 778.138	1
	54	53.5	0	275 720.420	7
	54	54.5	0	275 770.340	4
	54	53.5	1	274 618.778	2
	54	54.5	1	274 668.440	6
	54	53.5	2	273 518.538	−9
	54	54.5	2	273 567.930	−10
	55	54.5	0	280 711.405	3
	55	55.5	0	280 761.330	−7
	55	54.5	1	279 589.695	−9
	55	55.5	1	279 639.390	16
	55	54.5	2	278 469.438	−3
	55	55.5	2	278 518.848	2
	55	54.5	3	277 350.640	0
	55	55.5	3	277 399.773	−7
	56	55.5	0	285 701.178	8
	56	56.5	0	285 751.108	−10
	56	55.5	1	284 559.403	−8
	56	56.5	1	284 609.095	1

Table 4 continued

Isotope	N	J	v	Obs. (MHz)	Obs. −calc. (kHz)
	56	55.5	2	283 419.108	−4
	56	56.5	2	283 468.543	13
	56	55.5	3	282 280.308	7
	56	56.5	3	282 329.458	5
	56	55.5	4	281 143.008	2
	56	56.5	4	281 191.890	−4
	57	56.5	0	290 689.690	−7
	57	57.5	0	290 739.648	−9
$^{138}Ba^{37}Cl$	21	20.5	0	105 721.405	−6
	21	21.5	0	105 768.943	83
	21	20.5	1	105 390.230	3
	21	21.5	1	105 356.475	−28
	56	55.5	0	273 428.673	−2
	56	56.5	0	273 476.408	−42
	57	56.5	0	278 203.933	14
	57	57.5	0	278 251.738	32
	57	56.5	1	277 116.400	−2
	57	57.5	1	277 163.948	−24
	58	57.5	0	282 978.010	4
	58	58.5	0	283 025.788	−18
	58	57.5	1	281 871.700	−9
	58	58.5	1	281 919.335	44
$^{136}Ba^{35}Cl$	54	53.5	0	276 538.803	−24
	54	54.5	0	276 588.908	9
	55	54.5	0	281 544.590	28
	55	55.5	0	281 594.625	−21

ter. Reduced masses must then be calculated from ion masses rather than from masses of the neutral atoms. The remaining deviations seem to be real but effects of this order of magnitude are usually experienced even for $^1\Sigma$ molecules. No effect from the transfer of one electron mass can be observed for bromine or barium isotopic substitution simply because of the larger masses of these atoms.

Results of hyperfine structure measurements for $^{137}Ba^{35}Cl$ are listed in table 7. As to be expected from the small nuclear moments, hyperfine structure from the chlorine nucleus is not resolved. Calculations with estimated values for chlorine hfs parameters showed that no systematic line shifts will occur from unresolved chlorine hfs. Thus the hamiltonian for one coupling nucleus was used to fit the measured transition frequencies. b_ι D_0, γ_e and δ_γ were found to be in agreement with values calculated by mass relations from the

more precise $^{138}Ba^{35}Cl$ data. Therefore only the resulting hyperfine parameters have been listed in table 8.

5. Discussion

Hyperfine structure parameters for $^{137}Ba^{19}F$ and $^{137}Ba^{35}Cl$ are listed in table 8 with the data from matrix ESR [22] given for comparison. The values of the ^{137}Ba coupling constants b_1, c_1 and $(eqQ)_1$ determined from BaF and BaCl microwave measurements agree with each other within the quoted experimental errors. This is to be expected because of the very similar chemical bonding in these two molecules. Since the BaF values are more exact only these will be used in the following discussion. A comparison between matrix ESR and microwave results shows that the isotopic part of the magnetic interaction is slightly but significantly

Table 5

The molecular constants of $^{138}Ba^{35}Cl$. Constants for other isotopes may be calculated using the given reduced masses (see text)

	$^{138}Ba^{35}Cl$ this work	Previous work [38]
Y_{01} (MHz)	2517.27236(21)	2421.7
Y_{11} (MHz)	−10.02186(18)	−9.9
Y_{21} (kHz)	6.218(68)	
Y_{31} (kHz)	0.0411(95)	
Y_{02} (kHz)	−0.906041(32)	
Y_{12} (kHz)	−0.001124(19)	
Y_{03} (kHz)	−0.69 × 10^{-7}	
γ_{00} (MHz)	49.7183(98)	
γ_{10} (MHz)	−0.2650(25)	
γ_{01} (kHz)	0.0371(11)	
a_0 (cm^{-1})	2.332877(72) × 10^5	
a_1	−3.212015(60)	
a_2	6.4100(68)	
a_3	−9.114(64)	
ω_e (cm^{-1})	279.9179(49)	279.92(10)
$\omega_e x_e$ (cm^{-1})	0.8170(12)	0.785(3)
r_e (Å)	2.682765(10)	
μ (amu)[a]		
138/35	27.8953771	
138/37	29.1517032	
136/35	27.8125569	
137/35	27.8542461	

[a] Atomic masses taken from ref. [34].

higher in the matrix while the anisotropic part is lower. That means that hybridization of the unpaired electron orbital is slightly suppressed in the matrix, but these influences are quite small.

The quadrupole coupling constant measured for the ^{137}Ba nucleus seems to be surprisingly large when compared with $eqQ = -17$ MHz in BaO. Because of the highly ionic bond only two contributions to the electric field gradient have to be considered which can be clearly separated: Hybridization of the single unpaired

Table 6

Relative deviations from mass relations for $^{35}Cl/^{37}Cl$ substitution[a]

	Neutral atoms	Ionic bond
BaCl	1.7(3) × 10^{-6}	8.5(30) × 10^{-7}
CaCl	1.5(3) × 10^{-6}	6.5(30) × 10^{-7}
SrCl	1.5(5) × 10^{-6}	6.5(50) × 10^{-7}

[a] Atomic masses and electron mass from ref. [34].

Table 7

Transition frequencies $N+1 \leftarrow N, F+1 \leftarrow F$ of $^{137}Ba^{35}Cl$ in the ground vibrational state $v = 0$

N	F	Obs. (MHz)	Obs.–calc. (kHz)
20	18	105 612.23	7
	21	105 621.33	12
	19	105 629.81	−17
	20	105 631.60	−38
	20	105 642.47	5
	19	105 644.31	43
	21	105 652.81	25
	22	105 661.84	−41
53	51	271 126.77	31
	54	271 132.28	−84
	53	271 139.33	46
	52	271 149.25	13
	52	271 154.20	−64
	53	271 164.22	1
	54	271 171.21	71
	55	271 176.76	−5
54	52	276 126.30	72
	55	276 131.74	−38
	54	276 138.67	67
	53	276 148.37	−60
	53	276 154.13	65
	54	276 163.67	−223
	55	276 170.76	42
	56	276 176.35	82
55	53	281 124.59	9
	56	281 130.01	−47
	55	281 136.82	31
	54	281 146.45	−37
	54	281 152.80	70
	55	281 162.45	22
	56	281 169.15	−11
	57	281 174.61	−27

Table 8

Hyperfine structure parameters from $^{137}Ba^{19}F$ and $^{137}Ba^{35}Cl$ spectra (all constants are given in MHz)

	$^{137}Ba^{19}F$		$^{137}Ba^{35}Cl$
	this work	matrix ESR [22]	
$b_1 = b$ (Ba)	2301(9)	2401(6)	2314(9)
$c_1 = c$ (Ba)	75(6)	52(11)	96(20)
$(eqQ)_1 = eqQ$ (Ba)	−117(12)		−134(42)
$b_2 = b$ (F)	60(6)	59	
$c_2 = c$ (F)	−.	8	

valence shell electron and polarization of the closed shells. Both effects are due to the nearby F^- ion. The direct contribution of the ion field to the field gradient is small and may be neglected or added to the polarization of the closed shells;

$$eqQ = (eqQ)_{el} + (eqQ)_{pol}. \qquad (9)$$

The first term can be calculated from the anisotropic magnetic coupling constant c_1. Since c_1 and $(eqQ)_{el}$ are both proportional to $[(3\cos^2\theta - 1)/r^3]_{av}$ their ratio is given by

$$-c_1/(eqQ)_{el} = 3g_I \mu_0 \mu_N/e^2Q \approx 1.36, \qquad (10)$$

where μ_0 and μ_N are the Bohr and nuclear magneton, respectively, g_I is the g factor and Q the quadrupole moment of the ^{137}Ba nucleus. With the values of these constants taken from ref. [33] and the measured c_1 = 75(6) MHz we get $(eqQ)_{el} = -55(5)$ MHz and $(eqQ)_{pol} = -62(13)$ MHz. Thus more than 50% of the measured eqQ is due to the polarization of the closed shells. This result seems quite reasonable when compared with hyperfine structure in the CsF molecule which has been measured very precisely by molecular beam electric resonance [35]. Here only $(eqQ)_{pol}$ is present and it is easily calculated from the measured $eqQ = 1.2370$ MHz and the very small nuclear quadruple moment of -0.003×10^{-24} cm^3 that the field gradient from closed shell polarization is even larger than in BaF.

The wavefunction ψ of the unpaired electron may be described as

$$\psi = a_s \psi_{6s} + a_p \psi_{6p} + a_d \psi_{5d}, \qquad (11)$$

with $a_s^2 + a_p^2 + a_d^2 = 1$, if only admixture of 6p and 5d functions to the atomic 6s orbital is considered. a_s^2, a_p^2 and a_d^2 can be calculated by a comparison between molecular hyperfine structure parameters and experimentally determined magnetic and quadrupole coupling constants in the ^2S ground state and in ^2P and ^2D excited states of the $^{137}Ba^+$ ion. These constants have been determined by Becker et al. [37] and Höhle et al. [24] and are given in table 9.

Since the isotropic magnetic Fermi contact interaction comes only from s-electron contributions, a_s^2 is given by

$$a_s^2 = (b_1 + \tfrac{1}{3}c_1)/A(^2S) = 0.58. \qquad (12)$$

This shows the strong hybridization of the unpaired

Table 9
Hyperfine splitting factors of the BaII levels $^2S_{1/2}$, $^2P_{3/2}$ and $^2D_{3/2}$ (after refs. [24,37])

	6s $^2S_{1/2}$	6p $^2P_{3/2}$	5d $^2D_{3/2}$
A (MHz)	4014(4)	174(2)	263.4(12)
B (MHz)	–	96(2)	47(2)

electron in the field of the F^- ion. $(eqQ)_{el}$ is due to contributions from 6p and 5d admixture

$$(eqQ)_{el} = a_p^2 (eqQ)_{6p} + a_d^2 (eqQ)_{5d}. \qquad (13)$$

The atomic B values are defined as $B = eq_{n,j,j}Q$ while in the calculation of molecular eqQ values we have to use $q = q_{n,l,0}$ for $p\sigma$ and $d\sigma$ electrons. For $j = l + \tfrac{1}{2}$ these are related by [33]

$$q_{n,j,j} = q_{n,l,l} = -[(2l-1)/(l+1)]q_{n,l,0}. \qquad (14)$$

For $j = l - \tfrac{1}{2}$ we find using formula given by Kopfermann [36]

$$q_{n,j,j} = \frac{l-1}{l}\frac{R(j=l-\tfrac{1}{2})}{R(j=l+\tfrac{1}{2})}q_{n,l,l}$$

$$= -\frac{(l-1)(2l-1)}{l(l+1)}\frac{R(j=l-\tfrac{1}{2})}{R(j=l+\tfrac{1}{2})}q_{n,l,0}. \qquad (15)$$

$R(j=l-\tfrac{1}{2})$ and $R(j=l+\tfrac{1}{2})$ are relativistic corrections listed by Kopfermann. Using these formulas we get

$$(eqQ)_{6p} = -2B(^2P_{3/2}) = -192(4) \text{ MHz},$$

$$(eqQ)_{5d} = -1.77 B(^2D_{3/2}) = -83(4) \text{ MHz}.$$

Eq. (13) in combination with (12) and the normalization condition for the wavefunction then results in the coefficients listed in table 10. The errors in a_p^2 and a_d^2 are mainly due to the experimental errors in the determination of c. The good agreement of these con-

Table 10
Coefficients for 6s, 6p, 5d mixing in the wavefunction of the unpaired electron

	a_s^2	a_p^2	a_d^2
this work	0.580(3)	0.18(5)	0.24(5)
matrix ESR [22]	0.60	0.17	0.23

stants with those given by Knight et al. is remarkable because they have been obtained in a different way. Contribution of 6p and 5d orbitals to the magnetic coupling constant c has been calculated by Knight et al. using wavefunctions expressed as hydrogenic angular functions and Hartree—Fock radial functions. The coefficients a_p^2 and a_d^2 were then adjusted for best reproduction of the experimental coupling constants. The excellent numerical agreement is even more surprising because the c values from microwave spectra and matrix ESR differ considerably and the mixing coefficients depend rather critical on this quantity.

Charge distribution in these heavy and highly ionic molecules obviously depends on a delicate balance between many effects. The large 5d admixture to the wavefunction of the unpaired electron is favoured by the fact that 5d ^{2}D levels are only ≈ 5000 cm^{-1} above the 6s ^{2}S ground state but ≈ 15000 cm^{-1} below the 6d ^{2}P levels. Polarization of closed electron shells also plays an important role as demonstrated by the analysis of quadrupole hyperfine structure. An accurate theoretical treatment is thus expected to be very tedious. This may encourage further experimental efforts to provide more an better information, e.g. by a more precise determination of c or by measurements of the electric dipole moment in these molecules.

Acknowledgement

Note added in proof

Meanwhile we have got knowledge of a paper by Silverans et al. [39] in which an experimentally determined value of $B(5d\,^2D_{5/2})$ is given. This results in $(eqQ)_{5d} = -80.7(10)$ MHz in good agreement with the value calculated from $B(5d\,^2D_{3/2})$.

References

[1] T.C. Steimle, P.J. Domaille and D.O. Harris, J. Mol. Spectry. 68 (1977) 134.
[2] T.C. Steimle, P.J. Domaille and D.O. Harris, J. Mol. Spectry. 73 (1978) 441.
[3] M. Dulick, P.F. Bernath and R.W. Field, Can. J. Phys. 58 (1980) 703.
[4] L.E. Berg, L. Klynning and H. Martin, Physica Scripta 21 (1980) 173.
[5] P.F. Bernath, R.W. Field, B. Pinchemel, Y. Lefebvre and J. Schamps, J. Mol. Spectry. 88 (1981) 175.
[6] P.F. Bernath, P.G. Cummins and R.W. Field, Chem. Phys. Letters 70 (1980) 618.
[7] P.F. Bernath, B. Pinchemel and R.W. Field, J. Chem. Phys. 74 (1981) 5508.
[8] J.M. Brown, H. Martin and F.D. Wayne, Chem. Phys. Letters 55 (1978) 67.
[9] W.E. Ernst and T. Törring, Verhandlungen DPG 4 (1982) M53.
[10] R.N. Zare, A.L. Schmeltekopf, W.J. Harrop and D.L. Albritton, J. Mol. Spectry. 46 (1973) 37.
[11] P.F. Bernath, B. Pinchemel, R.W. Field, K. Möller and T. Törring, J. Mol. Spectry. 88 (1981) 420.
[12] P.J. Domaille, T.C. Steimle and D.O. Harris, J. Mol. Spectry. 66 (1977) 503.
[13] P.J. Domaille, T.C. Steimle and D.O. Harris, J. Mol. Spectry. 68 (1977) 146.
[14] J. Nakagawa, P.J. Domaille, T.C. Steimle and D.O. Harris, J. Mol. Spectry. 70 (1978) 374.
[15] Ch. Ryzlewicz and T. Törring, Chem. Phys. 51 (1980) 329.
[16] K. Möller, H.-U. Schütze-Pahlmann, J. Hoeft and T. Törring, Chem. Phys. 68 (1982) 399.
[17] H.-U. Schütze-Pahlmann, Ch. Ryzlewicz, J. Hoeft and T. Törring, Chem. Phys. Letters, to be published.
[18] W.J. Childs, D.R. Cok, G.L. Goodman and L.S. Goodman, J. Chem. Phys. 75 (1981) 501.
[19] W.J. Childs, D.R. Cok and L.S. Goodman, Can. J. Phys. 59 (1981) 1308.
[20] W.J. Childs, G.L. Goodman and L.S. Goodman, J. Mol. Spectry. 86 (1981) 365.
[21] W.J. Childs, L.S. Goodman and I. Renhorn, J. Mol. Spectry. 87 (1981) 522.
[22] L.B. Knight, W.C. Easley and W. Weltner Jr., J. Chem. Phys. 54 (1971) 322.
[23] W.E. Ernst and T. Törring, Phys. Rev. A25 (1982) 1236.
[24] C. Höhle, H. Hühnermann, Th. Meier and H. Wagner, Z. Physik A284 (1978) 261.
[25] T. Törring, J. Mol. Spectry. 48 (1973) 148.
[26] C.H. Townes and A.L. Schawlow, Microwave spectroscopy (McGraw-Hill, New York, 1955).
[27] R.S. Frosch and H.M. Foley, Phys. Rev. 88 (1952) 1337.
[28] B.R. Judd, Angular momentum theory for diatomic molecules (Academic Press, New York, 1975).
[29] H.E. Radford, Phys. Rev. A136 (1964) 1571.

[30] H. Appel, in: Landolt–Börnstein, Vol. 3 (Springer, Berlin, 1968).

[31] J.L. Dunham, Phys. Rev. 41 (1932) 721.

[32] R.M. Herman and S. Short, J. Chem. Phys. 48 (1968) 1266.

[33] W. Gordy and R.L. Cook, Microwave molecular spectra (Interscience, New York, 1970).

[34] A.H. Wapstra and K. Bos, At. Data Nucl. Data Tables 19 (1977) 177.

[35] T.C. English and J.C. Zorn, J. Chem. Phys. 47 (1967) 3896.

[36] H. Kopfermann, Kernmomente (Akademische Verlagsgesellschaft, 1956).

[37] W. Becker, W. Fischer and H. Hühnermann, Z. Physik 216 (1968) 142.

[38] H.W. Cruse, P.J. Dagdigian and R.N. Zare, Faraday Discussions Chem. Soc. 55 (1973) 277.

[39] R.E. Silverans, G. Borghs, G. Dumont and J.M. van der Cruyce, Z. Physik A295 (1980) 312.